frontiers | Frontiers in Coatings, Dyes and Interface Engineering

TYPE Brief Research Report
PUBLISHED 12 April 2024
DOI 10.3389/frcdi.2024.1379005

OPEN ACCESS

EDITED BY
Nadimul Haque Faisal,
Robert Gordon University, United Kingdom

REVIEWED BY
Zhenxue Zhang,
University of Birmingham, United Kingdom
Huatang Cao,
Huazhong University of Science and Technology, China

*CORRESPONDENCE
Richard Bailey,
Richard.bailey@dmu.ac.uk

RECEIVED 30 January 2024
ACCEPTED 21 March 2024
PUBLISHED 12 April 2024

CITATION
Bailey R and Sun Y (2024), Dry sliding wear and friction performance of zirconium dioxide tribopairs.
Front. Coat. Dye In. 2:1379005.
doi: 10.3389/frcdi.2024.1379005

Dry sliding wear and friction performance of zirconium dioxide tribopairs

Richard Bailey* and Yong Sun

School of Engineering and Sustainable Development, Faculty of Technology, De Montfort University, Leicester, United Kingdom

Zirconium is an attractive engineering material owing to its commendable temperature, corrosion resistance, and excellent biocompatibility. Despite these merits, its industrial applicability is hindered by elevated wear and friction in tribological settings. Previous research has concentrated on unmatched pair contacts involving zirconium and alumina primarily due to the exceptional hardness. However, there is a noticeable dearth of literature on the matched pair contact condition for zirconium dioxide. Thermal oxidation is a promising and cost-effective method to address the suboptimal tribological performance and enhance the mechanical and electrochemical properties of zirconium. In this study, thermal oxidation is employed to produce a 6-µm-thick oxide layer in an air furnace at 650°C for 6 h. Subsequently, the resulting surface coating was tribologically tested using a pin-on-disc tribometer against two distinct counterface materials, namely, alumina and zirconium dioxide, in a dry and unlubricated environment. The findings reveal that matched contact between the zirconium dioxide tribopair is unfavorable, leading to elevated friction and wear rates. Consequently, this configuration should be avoided in dry contact situations characterized by high contact pressures. However, under lower contact pressures, the wear performance is acceptable. Furthermore, when combined with lubrication, this system may have potential applications in bio-tribological systems.

KEYWORDS

zirconium, zirconium oxide, wear, friction, thermal oxidation

1 Introduction

Zirconium and zirconia have remarkable properties that make them suitable for various industrial applications. They can withstand elevated temperatures, resist corrosion, endure mechanical stresses (Zeng et al., 2024), and interact well with living tissues (Chevalier, 2006). These advantages have been exploited in the nuclear (Li et al., 2023), chemical processing (Webster, 1978), and biomedical (G et al., 2024) fields as well as for dental and orthopedic implants (Patil and Kandasubramanian, 2020; Bonnheim et al., 2021). However, galling is a concern when using zirconium in moving parts or applications in which metal-to-metal contact occurs under pressure and sliding conditions (Hofer and Ezzet, 2014; Kore et al., 2020). Galling is a form of severe adhesive wear that occurs when two metal surfaces adhere and deform, resulting in material transfer from one surface to the other.

Zirconium as a metal suffers from adhesive wear when in contact with other materials (Kim et al., 2014; Kumar et al., 2023). Surface treatments are often used to improve the tribological properties of zirconium, such as friction, wear, and lubrication. Some examples of surface treatments are ion implantation (Ryabchikov et al., 2018), laser surface

modification (Li et al., 2023), and thermochemical treatments (Ries et al., 2002; Pawar et al., 2011; Reger et al., 2018). Some of these treatments can result in zirconium dioxide (ZrO_2), a ceramic material with high mechanical strength and a wide range of industrial applications (Webster, 1978; Patil and Kandasubramanian, 2020; Kalyana Kumar and Sudersanan, 2021).

Thermal oxidation is an inexpensive and effective method of forming zirconium dioxide; this process involves heating zirconium in an oxygen-rich environment. Thermal oxidation can enhance the mechanical and electrochemical performances of zirconium by creating a protective layer of ZrO_2 on its surface (Alansari and Sun, 2017a). This type of surface treatment has been utilized for many years in orthopedic implants based on the commercial OXINIUM process (Pawar et al., 2011), which results in an approximately 5-μm-thick layer of ZrO_2 oxide.

The objective of this study is to investigate the wear mechanisms associated with the interactions between thermally oxidized zirconium and a zirconium dioxide ball, specifically under self-mating conditions. Currently, there is a limited body of literature addressing the contact behaviors in matched tribopairs. Conventional wisdom suggests avoiding matching contact due to potential surface adhesion issues, particularly for high solid solubility between surfaces (Maugis and Pollock, 1984). However, certain applications may derive benefits from matched contacts, including uniform wear behavior, consistent thermal expansion, and reduced galvanic coupling. Notably, the commercial availability of zirconium oxide bearings (comprising raceway and balls) attests to the advantages associated with such properties (Suh et al., 2008). The thermal oxidation process for commercially pure zirconium was implemented with parameters yielding an oxide layer thickness comparable to that achieved through the OXINIUM process. To assess its dry sliding performance, the matched contact pair was evaluated against an alumina counterpart to gauge the impact of heightened adhesive contact within the matched contact pair.

2 Methods

The base material, which was commercially pure zirconium (Zr) grade 2, with a purity of 99.2%, consisted of the following chemical components by weight: 0.16% oxygen (O), 0.025% nitrogen (N), 0.05% carbon (C), 0.005% hydrogen (H), 0.2% iron (Fe), and 0.2% hafnium (Hf), with the remaining portion being zirconium (Zr). This material was supplied by Goodfellow UK Ltd. and received in the form of a 1-mm-thick sheet that was subsequently cut into specimens measuring 20 mm × 15 mm. The specimens were manually ground using SiC grinding paper until they reached the P2400 grade, resulting in a surface finish of 0.14 μm (R_a). Following 10 min of ultrasonic cleaning in methanol, the specimens underwent thermal oxidation at 650°C for 6 h in an air furnace (CWF, Carbolite Gero). The samples were left to furnace cool, which resulted in an oxide layer of thickness 6 μm (Alansari and Sun, 2017b).

X-ray diffraction (XRD) was conducted with Cu-Kα1 radiation to determine the phases within the thermally oxidized samples. The metallographic cross sections of an oxidized specimen were cut, polished to a mirror finish, and etched using hydrofluoric acid (HF). The hardness of the cross section was measured using an Indentec ZHV microhardness tester with a load of 0.025 kg. Then, the physical and structural attributes of the specimens were examined under an optical microscope in both the cross-sectional and surface regions after undergoing wear testing.

To evaluate the dry sliding friction and wear characteristics, experiments were conducted using a pin-on-disk tribometer from Teer Coatings Ltd. The dry sliding tests were used to assess how the specimens responded to mechanical forces without the influence of corrosion or lubrication. During the dry sliding wear process, the disc specimen rotated against two types of balls, i.e., zirconium dioxide (ZrO_2) and alumina (grade 25 Al_2O_3), having 8 mm diameter each and supplied by Trafalgar Bearings Ltd.

Experiments were conducted under ambient conditions at 22°C by maintaining a constant rotational speed of 60 rpm over 3,600 s. Four different contact loads of 1 N, 3 N, 5 N, and 10 N were applied, corresponding to initial maximum Hertzian contact pressures of 367 MPa, 530 MPa, 627 MPa, and 791 MPa for the Zr–ZrO_2 interface, respectively. The diameter of the wear track was standardized to 9 mm, resulting in a sliding speed of 2.8 $cm \cdot s^{-1}$ and a cumulative sliding distance of 102 m for each trial. No lubrication was used during the tests, which were performed under ambient humidity conditions. The resulting wear track profiles were analyzed using a Taylor Hobson Intra Touch surface profilometer.

3 Results and discussion

After oxidizing the Zr samples, the thickness of the oxide layer was verified through cross-sectional examination. As illustrated in Figure 1A, the resulting surface layer exhibited a thickness of approximately 6 μm. The cross-sectional hardness measurements (Figure 1B) revealed greater hardness (~1,330 $HV_{0.025}$) within the oxide layer at the surface, consistent with ZrO_2 (Alansari and Sun, 2017b). The hardness profile also depicted a zone of increased hardness beneath the surface oxide that gradually transitioned to the initial hardness of untreated Zr (210 $HV_{0.025}$) at approximately 20 μm depth, which was attributed to oxygen diffusion.

XRD analysis confirmed the presence of monoclinic zirconium dioxide (m-ZrO_2) within the oxide layer, as expected for oxidation below 1,205°C (Baker and Okamoto, 1992; Reif et al., 2014). Figure 1C depicts the typical XRD patterns of untreated and oxidized Zr, indicating the presence of α-Zr from the substrate and monoclinic ZrO_2 from the surface oxide layer (OL), with no other phases detected.

The impacts of the contact load on the friction behaviors of untreated zirconium (Zr) and thermally oxidized zirconium (TO Zr) were investigated under dry sliding conditions against Al_2O_3 and ZrO_2 balls. The friction traces of contact against untreated Zr revealed a substantial and unstable friction coefficient for both counterface materials, as depicted in Figures 2A, B for the 5 N and 10 N loads, respectively. Microscopic examination of the untreated Zr revealed prominent signs of severe galling and plowing within the wear tracks, indicating the presence of high adhesive wear under dry sliding conditions and consistent with the findings of numerous prior studies (Alansari and Sun, 2017a; Alansari and Sun, 2019; Li et al., 2023).

The TO Zr displayed a nuanced response to sliding contact that was dependent on both the applied load and contact pair. The TO

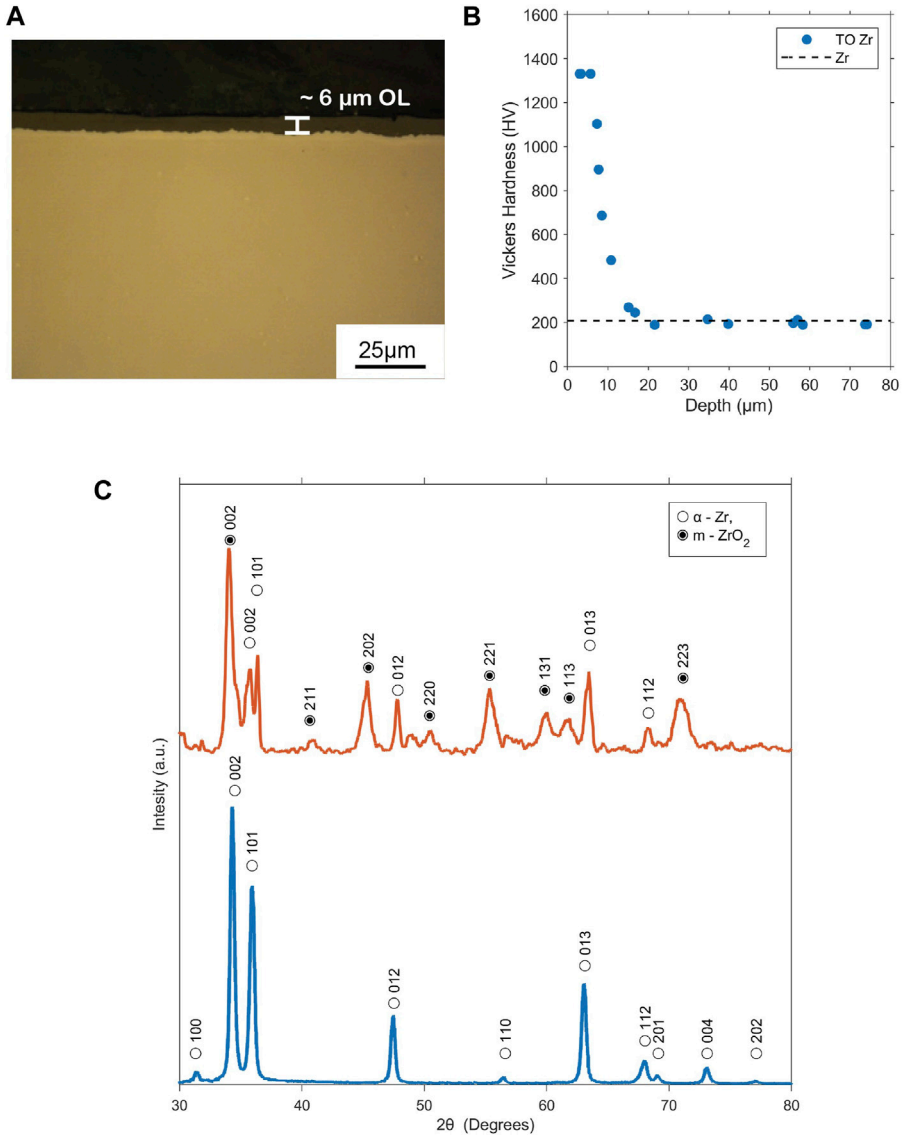

FIGURE 1
Characterization of zirconium that is thermally oxidized at 650°C for 6 h: **(A)** cross-sectional morphology, **(B)** hardness profile against depth from the surface, and **(C)** X-ray diffraction pattern.

$Zr–ZrO_2$ contact exhibited a higher coefficient of friction (CoF) than the untreated $Zr–ZrO_2$ contact across tests. These values are similar to those when ZrO_2 is in sliding contact with ZrO_2 (Suh et al., 2008). However, despite the higher CoF, the traces indicate a more stable CoF for TO $Zr–ZrO_2$ than untreated $Zr–ZrO_2$ at 5 N (Figure 2A). At the 10 N contact load, the difference in CoF between TO Zr and untreated Zr in contact with the ZrO_2 ball was negligible. The frictional response of TO $Zr–ZrO_2$ matched that of untreated $Zr–ZrO_2$ at approximately 2,500 s (Figure 2B), indicating failure and removal of the oxide layer in the contact zone.

Comparing untreated Zr and TO Zr in contact with Al_2O_3, the average CoF varied significantly with the applied contact load. For loads less than 5 N, the CoF for TO $Zr–Al_2O_3$ was below 0.2 (Figure 2C), producing a stable frictional response that was notably improved over that of the untreated $Zr–Al_2O_3$ configuration. At 5 N, the average CoF values were similar between the untreated Zr and Zr against Al_2O_3 ball. However, there was a noticeable difference in the frictional response, with TO $Zr–Al_2O_3$ gradually increasing throughout the test, while the untreated sample exhibited a characteristically spiky friction trace. At 10 N, the $Zr–Al_2O_3$ CoF values diverged, with the untreated value being lower than that of TO Zr in contact with the Al_2O_3 ball.

When investigating wear track morphology at 5 N, both TO contacts indicated that the oxide layer was in contact with the counterface material and was primarily affected by abrasive polishing (Figures 3C, D). Differences in the material transfer mechanisms were observed, where the ZrO_2 ball exhibited some transfer from the oxide layer of TO Zr (Figure 3C inset), while the Al_2O_3 ball showed no material transfer (Figure 3D inset). At higher magnification, the wear track of the TO $Zr–ZrO_2$ contact displayed numerous tensile cracks; although these were less pronounced in the

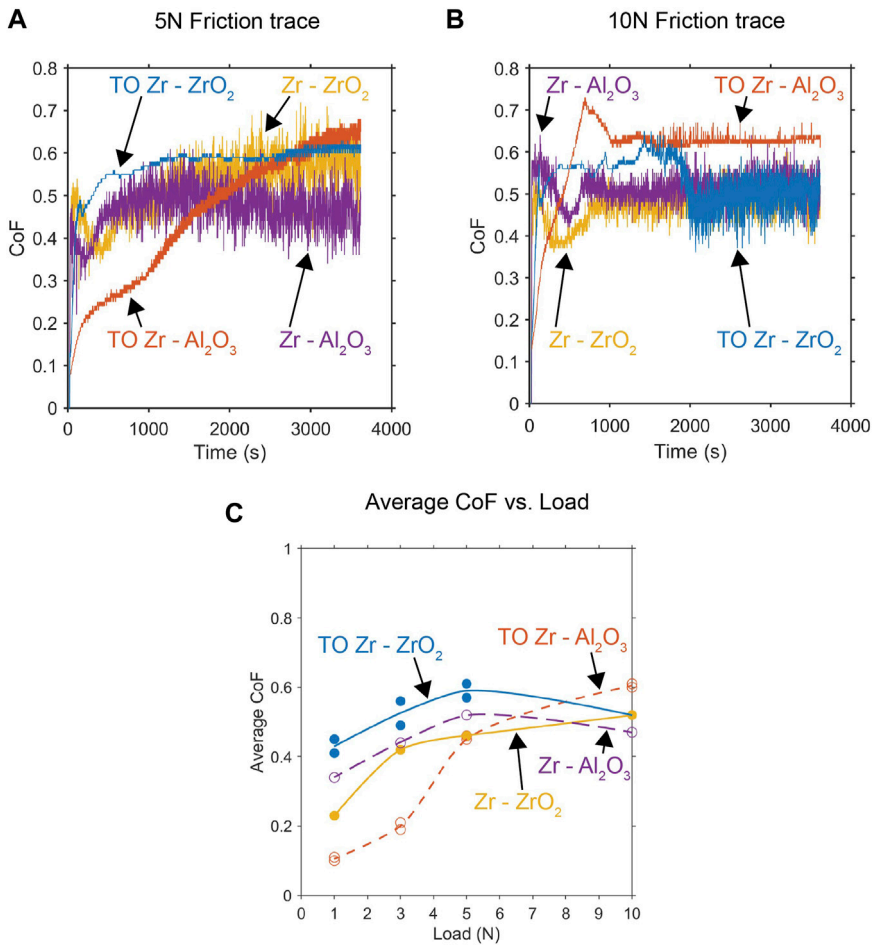

FIGURE 2
Recorded CoF traces for various contact couples under applied loads of **(A)** 5 N and **(B)** 10 N. **(C)** The load dependence of the recorded average CoF for each contact pair is also presented.

TO Zr–Al_2O_3 contact, they could still be observed at high magnifications.

Material loss due to sliding contact was assessed using a stylus profilometer. The wear track was divided into four sections around its circumference, and the volume loss in each section was averaged to determine the overall volume loss of the wear track. Additionally, the wear volume of the spherical counter material was assessed. The mean contact scar diameter calculations are presented in Figures 3A, B. The results indicate that the removal of the protective oxide layer in the 10 N load case, specifically in the TO Zr sample against ZrO_2 balls, led to accelerated wear. Both the ball and specimen experienced wear rates that were two orders of magnitude higher than those observed when in contact with alumina. When testing was performed at 5 N and below, the material loss of the treated samples was slightly higher for contact with the ZrO_2 counter body despite the high friction value. All results show that there are modest improvements in the CoF from oxidation treatment, but there are significant reductions in the amount of material removed during dry sliding contact.

The friction wear responses of the TO samples changed dramatically when the contact load was increased to 10 N for different counterface materials. The alumina contact exhibited a running-in period and then attained a steady CoF value of approximately 0.6 with frequent and sudden peaks in the friction trace (Figure 2B). The wear track morphology revealed extensive interfacial cracking, which was previously reported and attributed to the tensile failure of the oxide layer due to the high tractive force in the contact zone (Alansari and Sun, 2017b). The TO Zr–ZrO_2 contact pair exhibited an abrupt change in the frictional response. The initial response was similar to that observed at lower loads (high but stable friction) but was switched to a response identical to that of untreated Zr–ZrO_2 contact. This suggests that the oxide layer failed and was removed from the wear track, as confirmed by the microscopic investigations (Figure 3E), showing that the oxide layer was no longer present and that the subsurface Zr was in contact with the counter body. The wear track was characterized by gouging and adhesive wear, with significant material transfer between the wear track and ball (Figure 3E inset), for which energy-dispersive x-ray spectroscopy (EDS) investigations confirmed the presence of Zr on the counterface material. Figure 3G compares the wear track profiles observed under the 10 N contact load and clearly shows that the oxide layer was removed from the contact zone in the TO Zr–ZrO_2 contact pair. There is a belief that the heightened adhesive contact between the TO Zr–ZrO_2 tribological pair could have led to

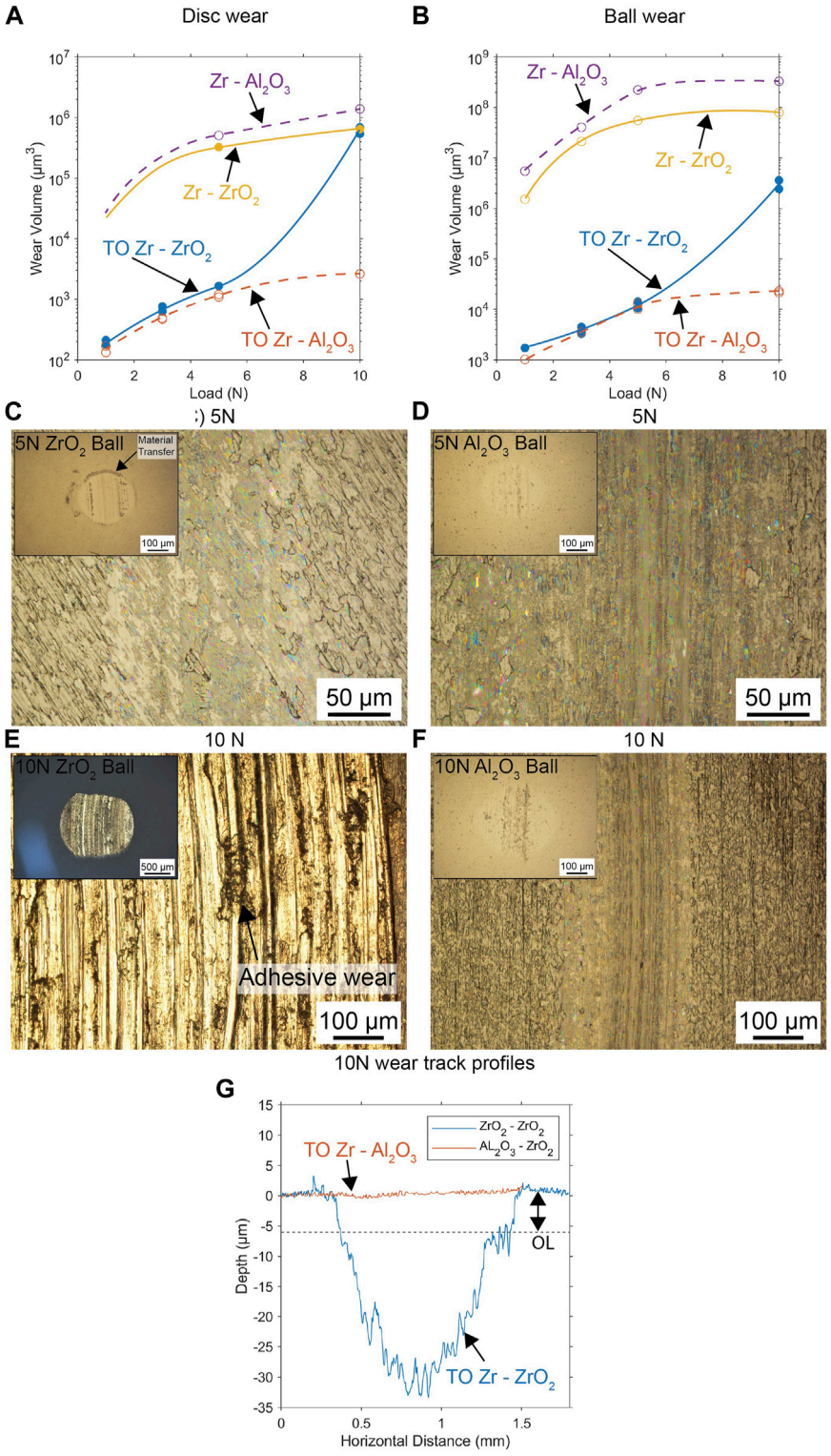

FIGURE 3
Recorded material volumes removed from the **(A)** disc and **(B)** balls under various loads and contact configurations. Optical micrographs in **(C)** and **(D)** depict the contacting surfaces under incremental load conditions and display the wear of the 5 N ball and disc contact for ZrO_2 and Al_2O_3, respectively. **(E,F)** Wear of the 10 N ball and disc for ZrO_2 and Al_2O_3, respectively. A comparison of wear track profiles is presented in **(G)** for the 10 N contact, highlighting the differences observed at higher contact loads.

premature failure and removal of the surface oxide compared to that observed in the unmatched TO Zr–Al_2O_3 (Figure 3F) contact scenario.

The wear mechanisms of the TO Zr–ZrO_2 contact were investigated through stop testing under an applied load of 10 N, whose results are depicted in Figure 4. The changes in the wear

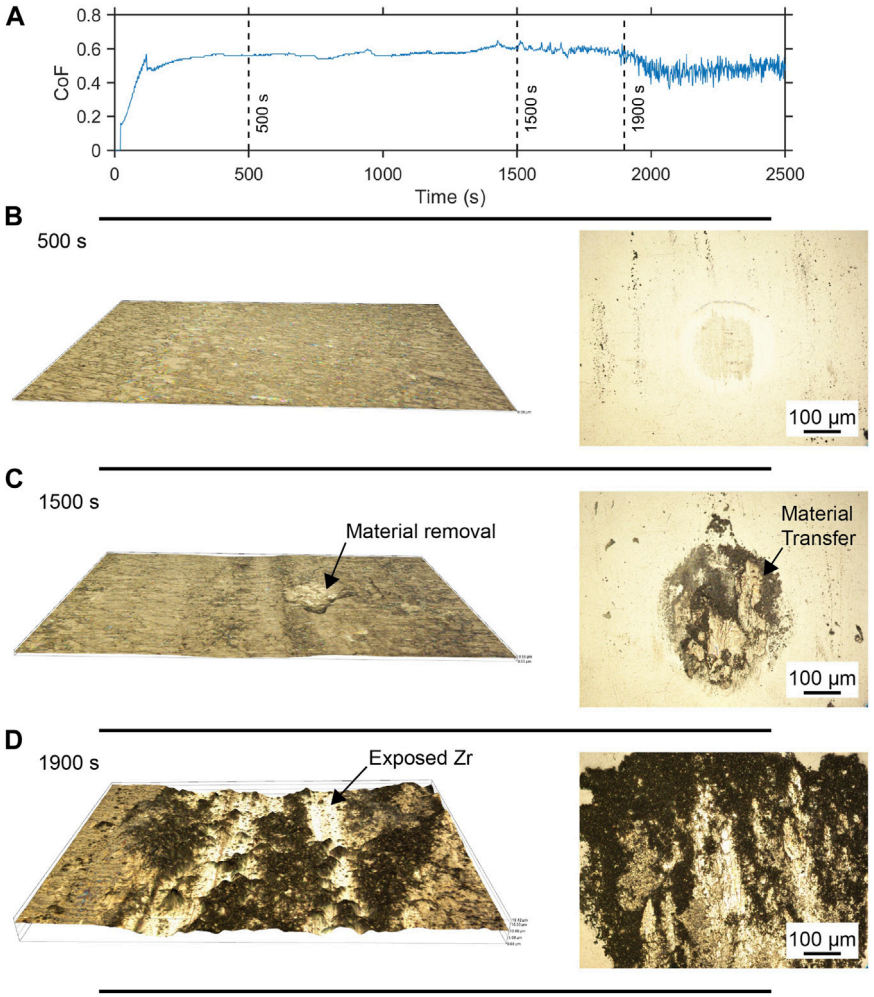

FIGURE 4
Friction/wear progression for TO Zr against ZrO_2. Enhanced view of the friction curve generated **(A)** during contact at 10 N with the 3D wear track (×200 magnification) and ball images (×200 magnification) at time intervals of **(B)** 500 s, **(C)** 1,500 s, and **(D)** 1,900 s. As sliding progresses, cohesive contact develops, resulting in breakdown and removal of the oxide layer.

track and counterface were examined as the sliding contact progressed. In the initial contact phase, the wear was caused by abrasive polishing, and minor wear was visible in the wear track and on the ball. However, some material transfer to the ball occurred, resulting in a rough texture at the center of the ball (Figure 4B). At this stage, there was no observable evidence of tensile cracking in the wear track. As the frictional response became more erratic, the wear track morphology showed some prominent features indicating that adhesive contact was a key factor in the wear evolution. The wear track showed obvious signs of tensile cracking, with observable material transfer from the wear track to the ball, as shown in Figure 4C. There were regions in the wear track where the oxide layer was pulled out from the surface and adhered to the counterface ball. The subsequent removal and impingement of the oxide layer caused an unstable friction CoF and accelerated oxide layer loss. Once this oxide layer removal was initiated, later stages showed that the contact mechanics of the wear track changed from OL–ZrO_2 ball contact to subsurface Zr–ball contact. During this transition to subsurface contact, the frictional response was a combination of third-body contact, OL–ZrO_2 contact, and Zr–ZrO_2 contact. As the OL was removed from the contact zone, the friction coefficient approached that of untreated Zr in contact with ZrO_2. The increased adhesion between the mating contact pair seemed to be the determining factor in the OL failure at a lower contact load.

It is evident that the TO Zr–ZrO_2 tribopair is undesirable and should be avoided in dry contact situations with high contact pressures. However, its wear performance is acceptable under lower contact pressures and might offer some potential for tribological systems when combined with lubrication.

4 Conclusion

1. Thermally oxidized Zr–ZrO_2 contact results in a high-friction contact pair (CoF ~0.58), which is akin to that observed when ZrO_2 surfaces are in contact with Al_2O_3 (CoF ~0.6). The friction of the protective surface is higher but more consistent than that observed when sliding against untreated Zr (CoF ~0.5). Although high CoF values are observed against both counterfaces, the low wear rates are encouraging, indicating that further investigations incorporating lubrication may be beneficial.

2. Thermally oxidized Zr–ZrO_2 contact exhibits low wear rate when tested below 10 N. The dominant wear mechanism here is that of abrasive polishing. At higher loads (exceeding 10 N), the protective surface is removed, with the wear mechanism being characterized by adhesive galling. Once the surface layer is withdrawn from the contact zone, the frictional response matches that of untreated Zr against ZrO_2.
3. Increased cohesion between the matched material contacts resulted in material transfer between the disc and ball, accelerating the removal of the ZrO_2 protective layer from the disc. The generation of microcracks in the wear track and subsequent cohesion are the primary mechanisms influencing the increased wear rate.

Data availability statement

The raw data supporting the conclusion of this article will be made available by the authors, without undue reservation.

Author contributions

RB: writing–original draft and writing–review and editing. YS: writing–original draft and writing–review and editing.

Funding

The author(s) declare that no financial support was received for the research, authorship, and/or publication of this article.

Conflict of interest

The authors declare that the research was conducted in the absence of any commercial or financial relationships that could be construed as a potential conflict of interest.

The author(s) declared that they were an editorial board member of Frontiers, at the time of submission. This had no impact on the peer review process and the final decision.

Publisher's note

References

Alansari, A., and Sun, Y. (2017a). A comparative study of the mechanical behaviour of thermally oxidised commercially pure titanium and zirconium. *J. Mech. Behav. Biomed. Mater.* 74, 221–231. doi:10.1016/j.jmbbm.2017.06.011

Alansari, A., and Sun, Y. (2017b). Effect of oxidation time on the tribological behavior of thermally oxidized commercially pure zirconium under dry sliding conditions. *Surf. Coatings Technol.* 309, 195–202. doi:10.1016/j.surfcoat.2016.11.070

Alansari, A., and Sun, Y. (2019). Surface finish effect on dry sliding wear behavior of thermally oxidized commercially pure zirconium. *Trans. Nonferrous Metals Soc. China* 29, 88–97. doi:10.1016/s1003-6326(18)64918-0

Baker, H., and Okamoto, H. (1992). *ASM handbook. vol. 3. alloy phase diagrams*.

Bonnheim, N. B., Van Citters, D. W., Ries, M. D., and Pruitt, L. A. (2021). Oxidized zirconium components maintain a smooth articular surface except following hip dislocation. *J. Arthroplasty* 36, 1437–1444. doi:10.1016/j.arth.2020.10.054

Chevalier, J. (2006). What future for zirconia as a biomaterial? *Biomaterials* 27, 535–543. doi:10.1016/j.biomaterials.2005.07.034

G, S. S., A, D., Adhikari, S., and N, R. (2024). Surface engineering of zirconium with chitosan PEDOT for enhanced bioactivity and corrosion behavior. *J. Alloys Compd.* 977, 173384. doi:10.1016/j.jallcom.2023.173384

Hofer, J. K., and Ezzet, K. A. (2014). A minimum 5-year follow-up of an oxidized zirconium femoral prosthesis used for total knee arthroplasty. *Knee* 21, 168–171. doi:10.1016/j.knee.2013.08.015

Kalyana Kumar, M., and Sudersanan, P. D. (2021). A study on thermomechanical properties of zirconium di oxide coated piston material of various thickness and its comparison with uncoated material. *Mater. Today Proc.* 45, 294–298. doi:10.1016/j.matpr.2020.10.650

Kim, J. H., Park, J. M., Park, J. K., and Jeon, K. L. (2014). Sliding wear and friction behavior of zirconium alloy with heat-treated Inconel718. *Nucl. Eng. Des.* 269, 66–71. doi:10.1016/j.nucengdes.2013.08.008

Kore, L., Bates, T., Mills, G., and Lybeck, D. (2020). Oxidized zirconium total knee arthroplasty implant failure in a patient with knee instability. *Arthroplasty Today* 6, 552–555. doi:10.1016/j.artd.2020.06.015

Kumar, B., Kumar, D., and Chaudhry, V. (2023). Tribological behavior of zirconium alloy against stainless steel under different conditions. *Tribol. Int.* 189, 108995. doi:10.1016/j.triboint.2023.108995

Li, J., Wang, H., Liu, K., and Jian, S. (2023b). Effect of laser power on the microstructure and property of ZrB2/ZrC *in-situ* reinforced coatings on zirconium alloy by laser cladding. *Vacuum* 213, 112104. doi:10.1016/j.vacuum.2023.112104

Li, Z., Guo, X., Zheng, M., Ren, Q., Cai, Z., and Jiao, Y. (2023a). Characterization and fretting wear behavior of zirconium alloy treated in high temperature water. *Wear* 532-533, 205078. doi:10.1016/j.wear.2023.205078

Maugis, D., and Pollock, H. M. (1984). Surface forces, deformation and adherence at metal microcontacts. *Acta Metall.* 32, 1323–1334. doi:10.1016/0001-6160(84)90078-6

Patil, N. A., and Kandasubramanian, B. (2020). Biological and mechanical enhancement of zirconium dioxide for medical applications. *Ceram. Int.* 46, 4041–4057. doi:10.1016/j.ceramint.2019.10.220

Pawar, V., Weaver, C., and Jani, S. (2011). Physical characterization of a new composition of oxidized zirconium–2.5wt% niobium produced using a two step process for biomedical applications. *Appl. Surf. Sci.* 257, 6118–6124. doi:10.1016/j.apsusc.2011.02.014

Reger, N. C., Balla, V. K., Das, M., and Bhargava, A. K. (2018). Wear and corrosion properties of *in-situ* grown zirconium nitride layers for implant applications. *Surf. Coatings Technol.* 334, 357–364. doi:10.1016/j.surfcoat.2017.11.064

Reif, M., Scherm, F., Galetz, M. C., and Glatzel, U. (2014). An enhanced three-step oxidation process to improve oxide adhesion on zirconium alloys. *Oxid. Metals* 82, 99–112. doi:10.1007/s11085-014-9479-2

Ries, M. D., Salehi, A., Widding, K., and Hunter, G. (2002). Polyethylene wear performance of oxidized zirconium and cobalt-chromium knee components under abrasive conditions. *J. Bone Jt. Surgery-American Volume* 84 (2), 129–135. doi:10.2106/00004623-200200002-00018

Ryabchikov, A. I., Kashkarov, E. B., Pushilina, N. S., Syrtanov, M. S., Shevelev, A. E., Korneva, O. S., et al. (2018). High-intensity low energy titanium ion implantation into zirconium alloy. *Appl. Surf. Sci.* 439, 106–112. doi:10.1016/j.apsusc.2018.01.021

Suh, M., Chae, Y., and Kim, S. (2008). Friction and wear behavior of structural ceramics sliding against zirconia. *Wear* 264, 800–806. doi:10.1016/j.wear.2006.12.079

Webster, R. T. (1978). Zirconium for chemical processing applications. *Met. Prog.* 113, 2.

Zeng, X., Zhang, C., Zhu, W., Zhu, M., Zhai, T., He, X., et al. (2024). Micro-scale mechanism for cyclic deformation behavior in zirconium under low-cycle-fatigue loading. *Int. J. Fatigue* 179, 108065. doi:10.1016/j.ijfatigue.2023.108065